ACS APPLIED MATERIALS & INTERFACES

Research Article

www.acsami.org

Hierarchically Porous Aminosilica Monolith as a CO_2 Adsorbent

Young Gun Ko,[†] Hyun Jeong Lee,[‡] Jae Yong Kim,[§] and Ung Su Choi*[,‡]

[†]Environmental Radioactivity Assessment Team, Korea Atomic Energy Research Institute, 989-111 Daedeok-daero, Yuseong-gu, Daejeon 305-353, Korea

[‡]Center for Urban Energy Systems, Korea Institute of Science and Technology, Hwarangno 14-gil 5, Seongbuk-gu, Seoul 136-791, Korea

[§]Department of Environmental Engineering, Chungbuk National University, 52 Naedong-ro, Heungok-gu, Cheongju, Chungbuk 361-763, Korea

ABSTRACT: A facile strategy is successfully developed for the centimeter-scale preparation of hierarchically porous aminosilica monolith as a CO_2 adsorbent just by simple processes of solvent-evaporation-induced coating, self-assembly, and concentration of tetraethyl orthosilicate sol on the surface of a polymer foam template without any adhesive composite material or hydrothermal treatment. (3-Aminopropyl) trimethoxysilane is immobilized on the surface of silica monolith via a gas-phase procedure. The silica frameworks of the monolith mimic those of the polymer foam template at the macroscale, and the frameworks are composed of the SBA-15 structure at the nanoscale. The hierarchically porous structure demonstrates improved properties over the single-mode porous component, with the macroporous framework ensuring mechanical stability and good mass transport properties, while the smaller pores provide the functionality for CO_2 adsorption.

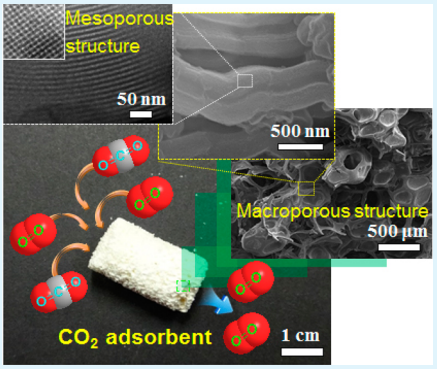

KEYWORDS: *hierarchical structures, aminosilica, porous materials, pressure drop, CO_2 capture*

1. INTRODUCTION

The CO_2 emissions associated with human activities are mainly due to the burning of fossil fuels and various chemical processes.[1] Currently, over 85% of the global energy demand is being supported by the burning of fossil fuels.[2] As the CO_2 levels in the atmosphere continue to increase, considerable concern has been raised regarding the impact of CO_2 emissions on the environment and its contribution to global climate change.[3] CO_2 capture is the most practical method to reduce CO_2 emission in the atmosphere.[4] In CO_2 capture processes, adsorption on solid media is considered as one of the most efficient methods owing to the regeneration with low energy.[5] In solid adsorbents, amines-modified porous materials have been found to be a viable option for effective CO_2 adsorbent owing to no corrosion of equipment, the adsorption/desorption process at atmospheric pressure, the low energy consumption for the adsorbent regeneration, the high adsorption capacity, and no loss of the adsorbent.[6−10]

Various types of amines-immobilized high surface area silica materials have been widely used for CO_2 capture.[11] However, despite the dramatic advantages of mesoporous materials, preparation of materials with simultaneous control of morphology and pore structure in different length scales still remains a challenging task.[12] Preparation of a hierarchically porous silica monolith (HPSM) has attracted much attention to make up for the weakness of the mesoporous silica materials as support materials.[13−18] In the HPSM structure, mesopores can provide adsorption sites for the CO_2 capture, whereas the existence of macropores can offer a highway for CO_2 accessing the sites with small pressure drops.[19] Therefore, fabrication of the HPSM has been the central core of researcher's interest. However, reported processes for fabrication of the HPSM demanded additional adhesive composite materials,[20] complicate process such as fabrication of highly ordered colloidal crystal template,[21] or a pressurizing process in an autoclave (hydrothermal treatment).[22] In these processes, complete removal of the template materials and additional adhesive composite materials is very important after the calcination process because the residual carbonaceous composites can cover the surface of HPSM and disrupt the immobilization of functional groups on the silica surface. In this study, HPSM has been fabricated simply just by processes of solvent-evaporation-induced coating, self-assembly, and concentration of tetraethyl orthosilicate (TEOS) sol on the surface of a polyurethane (PU) foam template without any adhesive composite material or complicate process. We were also able to freely manufacture the HPSM with the desired PU-template form.

As a functional group for CO_2 capture, (3-aminopropyl) trimethoxysilane (APTMS) was immobilized on the surface of HPSM (HPSM−NH_2) via a gas-phase procedure to increase the uniform surface density of amino groups on the silica surface.[23] HPSM−NH_2 showed higher CO_2 adsorption capacity than APTMS-immobilized SBA-15 at both room temperature (~25 °C) and high temperature (100 °C) because

Received: May 12, 2014
Accepted: July 7, 2014
Published: July 7, 2014

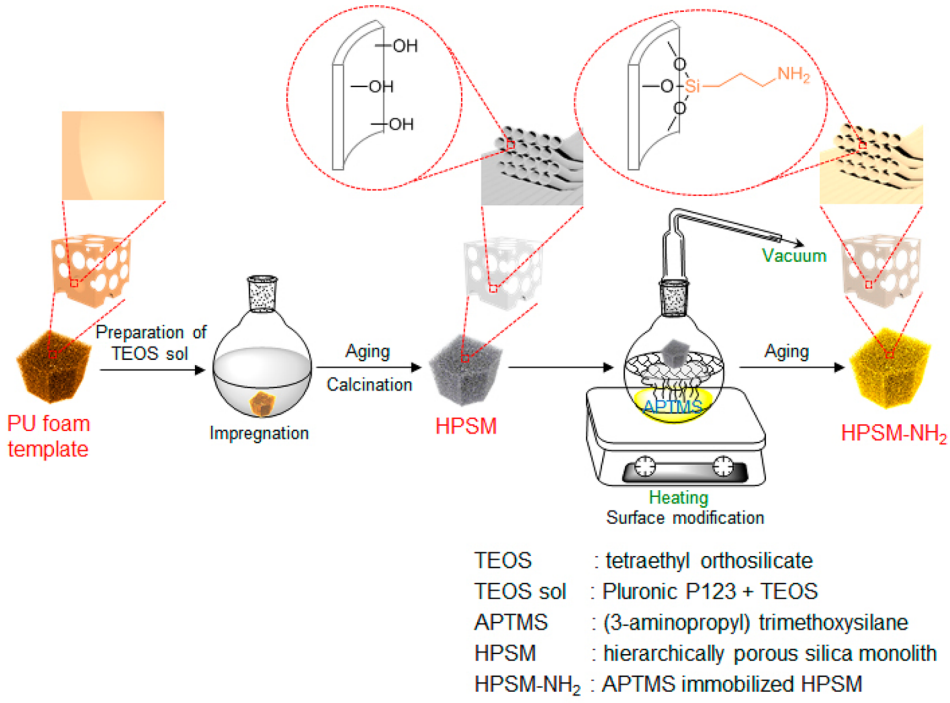

Figure 1. Schematic illustration of the preparation of the hierarchically porous aminosilica monolith (HPSM-NH_2).

the macropore in HPSM−NH_2 allows higher mass transport of CO_2 in the structure than the mesopore does. The pressure drop of the HPSM−NH_2 packed column was also approximately 36 times lower than that of the APTMS-immobilized SBA-15 packed column. In addition, molecular structure and composition information from the uppermost layers of the surface of HPSM−NH_2 were obtained by time-of-flight secondary ion mass spectrometry (ToF-SIMS).

In this study, we focused our efforts on development of the simple fabrication of a hierarchically porous aminosilica monolith to improve the CO_2 adsorption capacity, to make the CO_2 adsorbent for the desired shape and size, and to reduce the pressure drop in the CO_2 adsorption process.

2. EXPERIMENTAL SECTION

2.1. Reagents and Chemicals. All reagents and solvents were of AR grade and used without further purification unless otherwise noted. Polyurethane (PU) foam was purchased from LG sponge (Korea). Pluronic P123 triblock copolymer (EO_{29}−PO_{70}−EO_{20}), tetraethylorthosilicate (TEOS), and (3-aminopropyl) trimethoxysilane (APTMS) were bought from Aldrich. The 2 N HCl solution was purchased from Fluka. Deionized water (DI water) was obtained using a Milli-Q water system (18.2 MΩ·cm).

2.2. Preparation of Hierarchically Porous Silica Monolith (HPSM). HPSM was prepared from the prehydrolyzed TEOS, Pluronic P123, and a PU foam template. A 4.0 g amount of Pluronic P123 was dissolved in 30 g of DI water and 120 g of 2 N HCl solution, and the solution was well stirred for 5 h at 60 °C. Then, 8.5 g of TEOS was added slowly with stirring, and the resulting mixture was then kept at 24 h at 60 °C. Afterward, the clear supernatant liquid of the mixture solution was removed to concentrate the TEOS solution. The obtained solution was coated onto the PU foam template (1.5 × 1.5 × 1.5 cm^3). The air bubbles inside the PU foam template were removed by frequently squeezing the PU foam template during infusion of the concentrated sol solution. The infused PU foam template was kept in an 80 °C oven for 48 h followed by calcination with a nitrogen purge at 550 °C for 5 h to remove the Pluronic P123 and the PU template completely, and the hierarchically porous silica monolith was obtained. The silica monolith was named as HPSM.

2.3. Synthesis of Amino-Functionalized HPSM (HPSM-NH_2). APTMS was deposited onto HPSM using a gas-phase technique. Prior to deposition, the HPSM was pretreated at 150 °C in order to remove physisorbed water molecules from the silica surface. The pressure in the APTMS (5 mL) contained reactor was 10−50 mbar while vaporizing the APTMS. The APTMS in the reactor was vaporized at 120 °C for 24 h. The reaction temperature and reaction time were high enough to avoid condensation of the APTMS molecules onto the pore walls. For removal of unreacted reactants, the reaction was followed by a nitrogen purge at the reaction temperature. In addition, amino-functionalized HPSM was dried using a freeze drier (5 mTorr) for 1 week. The amino-functionalized silica monolith was named as HPSM−NH_2.

2.4. Characterization. High-resolution X-ray diffraction (XRD) patterns were obtained using a Rigaku D/max-2500 V/PC diffractometer with a high-power Cu Kα source (40 kV and 150 mA). Field emission gun scanning electron microscopy (FEG- SEM) measurements were taken on a FEI Inspect F50 at 15 kV. An elemental analyzer (EA 1108, FISONS Instruments) was used to measure the nitrogen amount of HPSM−NH_2. Transmission electron microscopy (TEM) images were obtained with a Philips CM-30 operating at 200 kV. Nitrogen adsorption/desorption isotherms were measured with an ASAP2420 sorption analyzer (Micromeritics). Prior to determination of the adsorption isotherm, the sample was evacuated at 1.333 Pa and 423.15 K for 2 h to remove all physisorbed species from the surface of the adsorbent. The Brunauer−Emmett−Teller (BET) method was used to determine the surface area. Pore size distributions were calculated by the Barrett−Joymer−Halenda (BJH) method. To analyze the surface of HPSM−NH_2, negative time-of-flight secondary ion mass spectrometry (ToF-SIMS) was carried out in the mass range of 0.5−400 m/z using an ION-TOF TOF-SIMS 5 system. Mass spectra were obtained using a Bi_3^+ liquid metal ion source (1 pA pulsed ion current) from an area of 100 μm × 100 μm. The mass resolution measured on the $Si^{\pm}$ signal of a silicon wafer was $m/\Delta m$ = 4000 in the negative mode. Fourier transform infrared (FT-IR) spectroscopy (Frontier, PerkinElmer) was used to confirm the synthesis of HPSM−NH_2. Samples were blended with KBr and then pressed into disks for analysis.

2.5. Carbon Dioxide Adsorption. CO_2 adsorption/desorption measurements for HPSM−NH_2 were performed using a thermogravi-

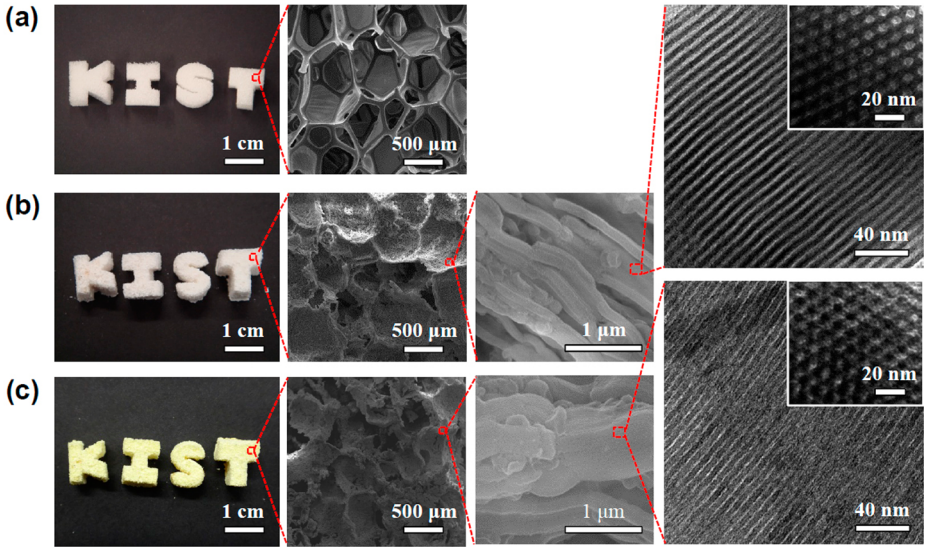

Figure 2. Representative photograph, FEG-SEM, and TEM images of the hierarchically porous structures from low magnification to high magnification. (a) PU foam template, (b) hierarchically porous silica monolith (HPSM), and (c) APTMS-immobilized HPSM (HPSM−NH_2).

metric analyzer (TGA). A sample weight of ca. 10 mg was loaded into an alumina sample pan in a TG unit (SCINCO thermal gravimeter S-1000) and tested for CO_2 adsorption/desorption performances. Initial activation of the samples was carried out at 110 °C for 3 h in a nitrogen atmosphere. An adsorption run was then conducted using dehumidified CO_2 gas (99.9%, Shinyang Oxygen Industry Co., Korea) at 28, 50, 75, and 100 °C under atmospheric pressure, and the desorption pressure was performed at 110 °C for 3 h. Both CO_2 and N_2 were passed through an automatic valve, assisted with a timer for continuous adsorption and desorption profile. The silica gel blue (Daejung Chemicals Co., Korea) packed columns were used to remove the moisture in CO_2 and N_2 gases.

2.6. Pressure Drop Measurement. In pressure drop experiments, 0.45 g of HPSM−NH_2 was packed into the adsorption column (i.d. 7.6 mm × length 80 mm). A 0.45 g amount of SBA-15-NH_2 was used for comparison (i.d. 7.6 mm × length 60 mm). The pressure drop between the inlet and the outlet of the column was measured under various velocities of dehumidified CO_2 gas (0−0.15 m/s) at a room temperature.

3. RESULTS AND DISCUSSION

3.1. Synthesis of HPSM−NH_2. Formation of amino-functionalized HPSM (HPSM−NH_2) was fabricated using the process of solvent-evaporation-induced self-assembly. The process is mainly composed of five steps: preparation and concentration of TEOS sol, impregnation of polyurethane (PU) template, aging and calcination, surface modification, and aging (Figure 1). In the first step, Pluronic P123 triblock copolymer (EO_{29}−PO_{70}−EO_{20}) forms a cylindrical micelle structure, and TEOS adsorbs onto the cylindrical micelle structure (CMS). In the second step, TEOS/CMS composite adsorbs onto the surface of the PU foam template. In the third step, solvent evaporation (induced coating and self-assembly) occurs and hierarchically porous silica monolith (HPSM) forms after calcination. In the fourth step, aminosilane (APTMS) is deposited onto HPSM through a gas-phase technique. After deposition of aminosilane on the surface of HPSM, individual aminosilane can incorporate with the surface of HPSM via (i) covalent bonding with attached aminosilanes on HPSM, (ii) direct covalent bonding with HPSM, (iii) multilayer formation with neighboring aminosilanes by vertical and horizontal polymerization, (iv) intermolecularly hydrogen bonding with amine group or HPSM surface silanol group, and (v) noncovalent bonding such as ionic or electrostatic attraction. For regeneration of the CO_2 adsorbent, the structure of v should be avoided because the structure is too weak to endure the regeneration process.[24−27] This causes loss of CO_2 adsorption capacity of the adsorbent during the CO_2 adsorption−desorption cycling process. Therefore, deposition was followed by a nitrogen purge at the deposition temperature and freeze drying under vacuum for removal of unreacted aminosilanes. In the final step, the deposited aminosilane binds to the surface of HPSM tightly and forms a covalent bond.

The significant advantage of our hierarchically porous silica monolith (HPSM) is that the monolith can be made in almost any shape. It depends only on the shape of the template. In this study, a PU foam was used as the template. The first initials of the rersearch inistitute (KIST, Korea Institute of Science and Technology) was fabricated in three dimensions with the PU foam as shown in Figure 2a. The range of the pore size in the PU foam template is 300−800 μm. After the processes of solvent-evaporation-induced self-assembly of the TEOS sol solution, aging, and calcination, the walls of the giant pores (300−800 μm) had an open periodic mesoporous structure which was confirmed by transmission electron microscopy (TEM) images (Figure 2b). Highly ordered parallel lines were able to be observed in the TEM image, relating to a hexagonal arrangement of mesopores (side view). In the inset images, the uniform hexagonal mesostructure could be seen from the perpendicular view to the pore channel axis. An intricate, well-ordered meso−macroporous solid, in which all pore scales are interconnected, was produced via solvent-evaporation-induced self-assembly of the TEOS sol solution, aging, and calcination. Even after deposition of the aminosilane (APTMS) onto the surface of the HPSM, all meso−macropores were well interconnected as shown in Figure 2c.

The N_2 adsorption/desorption isotherms of HPSM and HPSM−NH_2 are presented in Figure 3a. All samples showed a typical type IV N_2 adsorption isotherm with pronounced capillary condensations reflecting internal mesopores and interparticle voids between the primary particles.[28] However, each sample showed different hysteresis. The HPSM displayed a type of IV isotherm with H1 hysteresis and a sharp increase in

dx.doi.org/10.1021/am5029022 | ACS Appl. Mater. Interfaces 2014, 6, 12988−12996

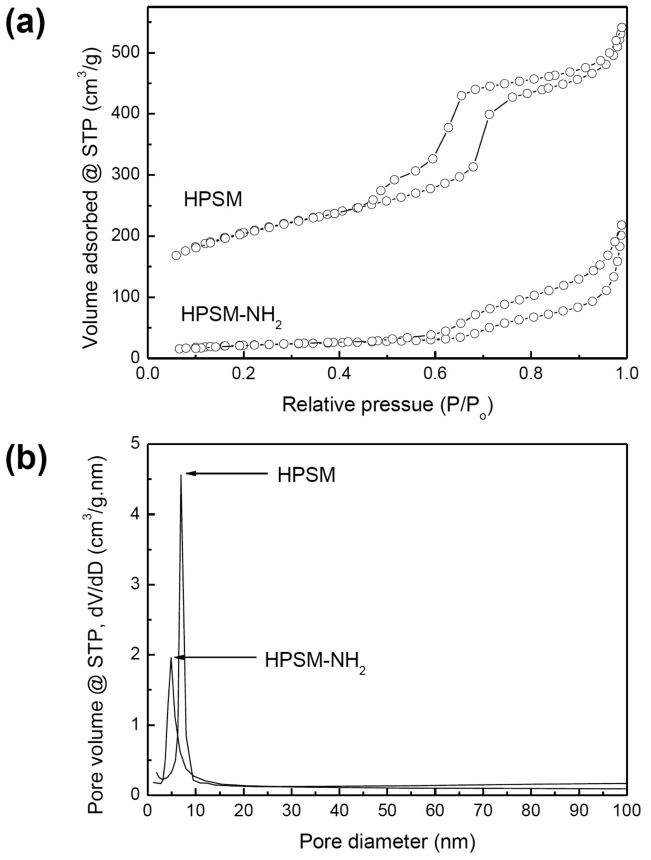

Figure 3. Textural characterization of hierarchically porous silica monoliths. (a) N_2 adsorption/desorption isotherms, and (b) pore size distributions of HPSM and HPSM−NH_2.

volume adsorbed at $P/P_o \approx 0.68$, characteristic of highly ordered mesoporous materials. However, capillary condensation of N_2 occurred over a slightly wider P/P_o range in APTES-functionalized HPSM (HPSM−NH_2) than in HPSM because of heterogeneous mesopores in HPSM−NH_2. After surface functionalization of HPSM, the surface of the mesopores in HPSM became heterogeneous while the surface of mesopores in unmodified HPSM was homogeneous. The HPSM pore diameter distribution showed a narrow pore size distribution as shown in Figure 3b. However, HPSM−NH_2 showed slightly broader and lower intensity than HPSM in the pore size distribution curves. The textural properties of the samples are summarized in Table 1. HPSM presented a high value of specific surface area (726. 40 m^2/g) and 8.38 nm pore diameter. HPSM−NH_2 showed lower values of textural properties (specific surface area 312.15 m^2/g, pore diameter: 5.26 nm) than HPSM.

Structural characterization by X-ray diffraction (XRD) reveals that the frameworks of HPSM are composed of the ordered mesoporous arrangement of the typical SBA-15 structure (Figure 4). The XRD pattern at low angle corresponding to

Table 1. Textural Properties of APTMS Immobilized HPSM and SBA-15

materials	specific surface area (BET) [m^2/g]	pore diameter (BJH) [nm]
HPSM	726	8.38
HPSM−NH_2	312	5.26
SBA-15	873	5.29
SBA-15−NH_2	288	3.09

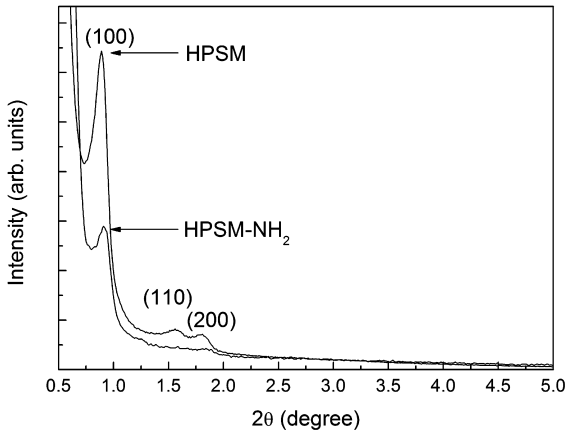

Figure 4. XRD patterns of HPSM and HPSM−NH_2.

the HPSM shows a typical profile of a 2D-hexagonal structure with *P6mm* plane group of SBA-15. The XRD pattern of HPSM displays a very intense peak (100) and two additional high-order peaks (110, 200). This XRD pattern reveals that the wall of HPSM consists of the hexagonal structure of SBA-15.[29] The hexagonal structure was clearly shown in the TEM image of HPSM (see Figure 2b). It should be noted that the decrease in (100) intensity for HPSM−NH_2 provides evidence of APTMS grafting occurring mainly inside the mesopore channels, since attachment of APTMS to the surface of the mesopore channels reduces the XRD intensity of the amorphous silica wall.

Incorporation of the aminosilane in the silica frameworks can be qualitatively confirmed by the FT-IR spectra shown in Figure 5. To remove adsorbed gas and water molecules, HPSM

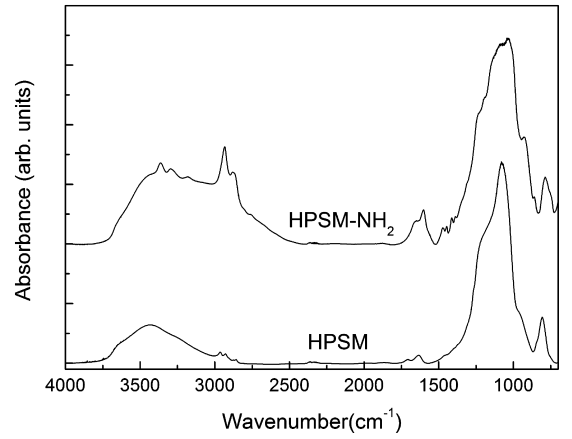

Figure 5. FT-IR spectra of HPSM and HPSM−NH_2.

and HPSM−NH_2 were dried at 110 °C under vacuum for 3 days and quickly analyzed with a FT-IR spectrometer. After modifiaction of HPSM with APTMS (HPSM−NH_2), the new peaks appeared at 3358, 3297, 2935, 2882, and 1603 cm^{-1} for NH_2 asymmetric stretching, NH_2 symmetric stretching, CH_2 asymmetric stretching, CH_2 symmetric stretching, and NH_2 deformation, respectively. The newly appearing peaks demonstrate that APTMS was successfully immobilized on the surface of HPSM.

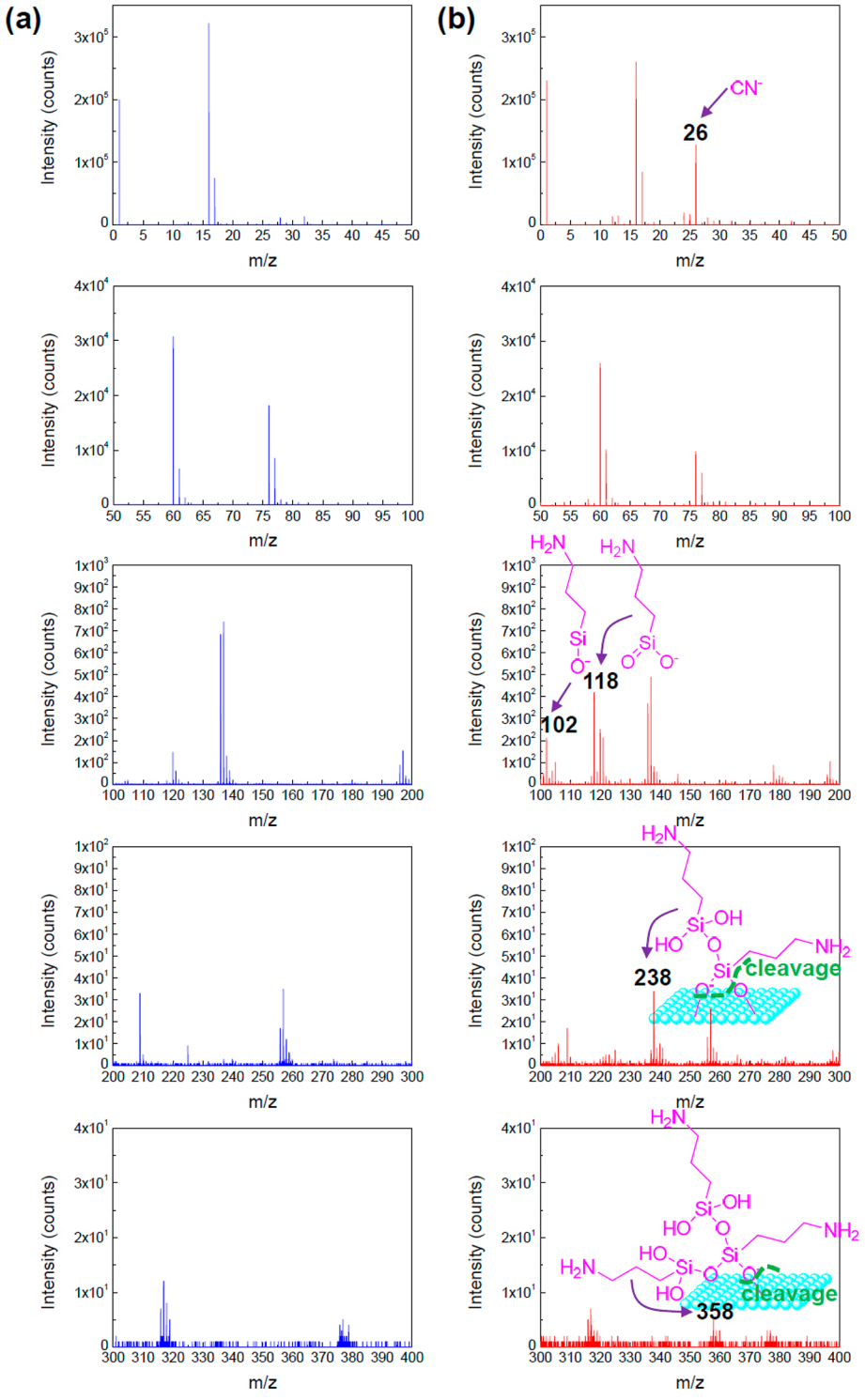

Figure 6. Negative ToF-SIMS spectra of (a) HPSM and (b) HPSM−NH_2.

3.2. Surface Characterization of HPSM−NH_2 with ToF-SIMS. After immobilization of APTMS on HPSM, the pore diameter of mesopores in HPSM decreased from ca. 8.38 to ca. 5.26 nm (see Table 1). Therefore, the increased wall thickness of the mesopores is ca. 1.56 nm. If APTMS is immobilized on the surface of the HPSM as a monolayer state, maximum increased thickness of HPSM−NH_2 is approximately 0.9 nm theoretically due to the ca. 0.9 nm of the APTMS molecular length.[30] This result indicates that APTMS multilayers were incorporated onto the surface of HPSM. ToF-SIMS technique provides molecular structure and composition information from the uppermost layers of surfaces. Negative-ion ToF-SIMS spectra of HPSM and HPSM−NH_2 are shown in Figure 6. After immobilization of APTMS on the surface of HPSM (Figure 6b), the major peaks at m/z 26, 102, and 118 amu correspond to CN^-, $C_3H_8ONSi^-$, and $C_3H_8O_2NSi^-$, respectively. These fragments are the APTMS fingerprints, since they are present in the spectrum due to fragmentation of the APTMS molecule. Interestingly, the specific peaks appearing at 238 and 358 amu correspond to the fragments of the

dx.doi.org/10.1021/am5029022 | ACS Appl. Mater. Interfaces 2014, 6, 12988−12996

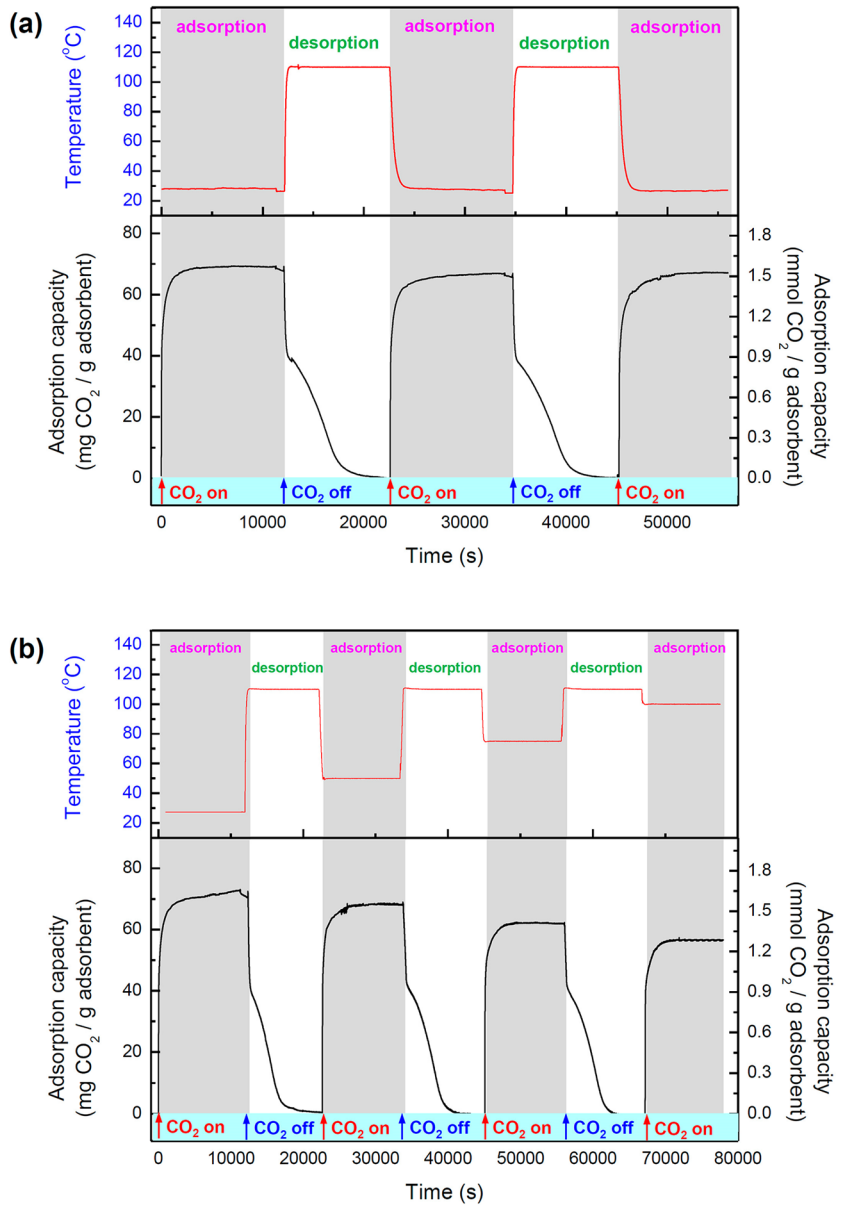

Figure 7. CO_2 adsorption/desorption cycles on HPSM−NH_2 (a) at isothermal adsorption temperature and (b) at different adsorption temperatures (28, 50, 75, and 100 °C).

polyaminosilanes. These peaks indicate that the APTMS multilayer formation owing to horizontal and vertical polymerization formed during immobilization of APTMS on the surface of HPSM.

3.3. CO_2 Adsorption/Desorption on Modified HPSM. To evaluate the CO_2 adsorption capacity on HPSM−NH_2, the repeated CO_2 adsorption/desorption performances were conducted. The adsorption performance was carried out at 28 °C at atmospheric pressure with pure CO_2 gas, and the desorption performance was conducted at 110 °C at atmospheric pressure with N_2 gas. In this adsorption/desorption performance, the maximum CO_2 adsorption value (1.51 mmol/g) was stable during the cycle process owing to complete removal of CO_2 from HPSM−NH_2 in the desorption process (Figure 7a). The percentage loss of adsorption capacity of HPSM−NH_2 was less than 1% for 3 cycles. Sayari et al. reported the high loss of adsorption capacity was observed in the case of CO_2 adsorption−desorption cycling experiment under dry conditions, while the loss was very low under humid conditions.[10,31] Although we did only 3 cycles for the adsorption−desorption cycling experiment, the loss was very low under dry conditions. HPSM−NH_2 did not exhibit high adsorption capacity; however, it showed good stability of the regeneration under dry conditions.

To compare the value of the maximum CO_2 adsorption capacity of HPSM−NH_2 with other CO_2 adsorbent, APTMS-immobilized SBA-15 (SBA-15−NH_2) was prepared according to our previous report.[32] Textural properties (specific surface area and pore diameter) of the synthesized SBA-15 and SBA-15−NH_2 are summarized in Table 1. Surface properties of HPSM−NH_2 and SBA-15−NH_2 as a CO_2 adsorbent are listed in Table 2. The number of APTMS molecules in HPSM−NH_2 was calculated using the loaded amount of nitrogen (3.78 mmol/g) and the BET specific surface area of HPSM and SBA-15 for HPSM−NH_2 and SBA-15−NH_2 respectively, and the values for HPSM−NH_2 and SBA-15−NH_2 were 3.13 and 2.31

dx.doi.org/10.1021/am5029022 | ACS Appl. Mater. Interfaces 2014, 6, 12988−12996

Table 2. Comparison of APTMS Immobilized HPSM and SBA-15

materials	N amount in adsorbent [mmol/g]	no. of molecules (APTMS) per area [#/nm^2]	adsorption capacity of CO_2 [mmol/g]	adsorbed CO_2 per N [mmol/mmol]
HPSM−NH_2	3.78	3.13	1.51	0.39
SBA-15−NH_2	3.43	2.31	0.95	0.27

#/nm^2 respectively. Primary amine can incorporate with CO_2 to make carbamate via the zwitterionic intermediate formation. Caplow reported carbamate formation through the zwitterionic intermediate, and other research groups developed it.[33] The mechanism was later summarized well by Choi et al. that the lone pair on the amine attacks the carbon of CO_2 to produce the zwitterion, and then free base deprotonates the zwitterion to form the carbamate.[5] Thus, the maximum amine efficiency of an amine adsorbent is 0.5 mol of CO_2 per mol of N under dry conditions. In addition to amine groups for the CO_2 capture agent, a hydroxyl group on the silica surface can influence CO_2 adsorption.[34−38] Amine efficiency, defined here as the number of CO_2 captured per mass unit divided by the moles of N per mass unit, gives a reflection of the adsorbent's efficiency in perspective with its potential. Here, the CO_2 adsorption performance was conducted at dry conditions, and the amine efficiency of HPSM−NH_2 was 0.39 mmol/mmol. In theory, CO_2 incorporates with two primary amines at dry conditions.[39] However, the obtained amine efficiency of the HPSM−NH_2 indicated a lower value than 0.5 of the theoretical one. The geographical and steric effects can cause isolation of some amines, which can serve the role of CO_2 capturing. Therefore, the adsorption capacity value from the CO_2 adsorption experiment is lower than the theoretical one. However, the value of HPSM−NH_2 is higher than that of SBA-15−NH_2 owing to the hierarchically porous structure of HPSM−NH_2. The macropore allows higher mass transport of CO_2 in the structure than the mesopore does.

Figure 7b shows the CO_2 adsorption/desorption cycles of HPSM−NH_2 at different adsorption temperatures. It can be observed that the CO_2 adsorption capacity of HPSM−NH_2 at 100 °C (1.28 mmol/g) is lower than that at 28 °C (1.51 mmol/g). Adsorption of CO_2 on the porous adsorbent consists of two steps: (i) CO_2 adsorption on the surface of adsorbent and (ii) CO_2 diffusion from the surface into the pores of the adsorbent. Thermodynamic and dynamic factors are the main parameters influencing the adsorption capacity.[40] However, these factors are mutually vying. Increasing the temperature has both positive and negative influences on the CO_2 adsorption capacity, that is, to enhance the diffusion of CO_2 favoring adsorption but to enhance decomposition of ammonium carbonate disfavoring adsorption. Although the increase of the adsorption temperature is not favorable to enhancement of the CO_2 adsorption capacity of HPSM−NH_2, its CO_2 adsorption capacity is less influenced by the temperature than that of previously reported SBA-15−NH_2 due to hierarchical pores in its structure for good CO_2 diffusion.[32] Therefore, this result leads to the conclusion that CO_2 diffusion is not the dominant parameter reducing CO_2 adsorption on HPSM−NH_2 in comparison to the thermodynamic factor.

3.4. Pressure Drop. Pressure drop is one of the significant parameters in industrial processes. Macropores in hierarchically porous structures would provide easier access to the active sites and reduce the pressure drop over the materials.[41−45] Figure 8 shows the pressure drop across packed beds of HPSM−NH_2 and SBA-15−NH_2 at various superficial velocities. The pressure drop per unit length was calculated by dividing the experimental results over the length of the corresponding bed. It can be anticipated that components possessing hierarchical porosity demonstrate to possess improved properties over single-mode porous components, with the macroporous framework ensuring mechanical stability and good mass transport properties (such as a higher rate of external transfer of mass and lower pressure drop), while the smaller pores provide the functionality for CO_2 adsorption. This was confirmed by the low pressure drop recorded per unit length of bed of HPSM−NH_2, which was approximately 36 times lower than the pressure drop per unit length of bed of SBA-15−NH_2.

4. CONCLUSIONS

In summary, we demonstrated the facile fabrication of hierarchically porous aminosilica monolith (HPSM−NH_2) as a CO_2 adsorbent using the PU foam template, tetraethyl orthosilicate (TEOS), triblock copolymer (Pluronic P123), and

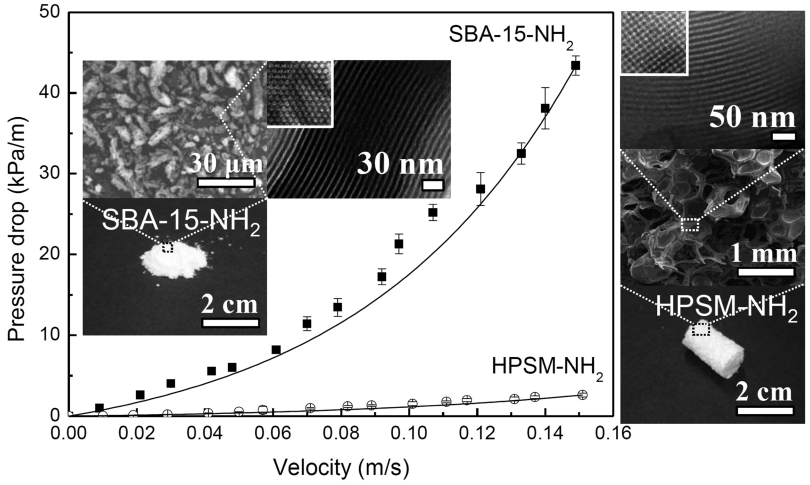

Figure 8. Pressure drop along adsorption columns packed with SBA-15−NH_2 and HPSM−NH_2 (insets; photograph, FEG-SEM, and TEM images of used SBA-15−NH_2 and HPSM−NH_2 for the CO_2 adsorption column). Data are presented as mean ± standard deviation, n = 5.

(3-aminopropyl) trimethoxysilane (APTMS). Hierarchically porous silica monolith (HPSM) was fabricated simply just by solvent-evaporation-induced coating, self-assembly, and concentration of TEOS sol on the surface of the polyurethane (PU) template without any adhesive composite material or pressurizing process. We were able to freely manufacture the hierarchically porous aminosilica monolith with the desired PU-template shape. APTMS was immobilized on the surface of HPSM (HPSM−NH_2) via a gas-phase procedure to increase the surface density of amino groups on the silica. It was confirmed by TEM and XRD analysis that the walls of macropores in HPSM, the silica frameworks, are composed of SBA-15. ToF-SIMS results indicated that the multilayers owing to APTMS polymerization occurred during immobilization of APTMS on the surface of HPSM (HPSM−NH_2), although monolayers also formed on the surface. These multilayers can influence the CO_2 adsorption capacity of HPSM−NH_2. The prepared HPSM−NH_2 showed not only slightly higher CO_2 capture amount but also slightly higher efficiency for CO_2 capture than SBA-15−NH_2. The synthesized HPSM−NH_2 depends on the adsorption temperature that the CO_2 adsorption capacity of HPSM−NH_2 was high at the low adsorption temperature. The purpose behind the design of the hierarchically porous structure is to improve the flow resistance and pressure drop. It is noteworthy that the pressure drop of HPSM−NH_2 was approximately 36 times lower than that of SBA-15−NH_2.

The prepared HPSM can be a promising support for immobilization of functional groups for specific purposes. We believe that our HPSM−NH_2 can be applied to various applications such as CO_2 capture, sequestration of heavy metal ions, radionuclides capture, etc.

AUTHOR INFORMATION

Corresponding Author

*Phone: 82-2-958-5657. Fax: 82-2-958-5659. E-mail: uschoi@kist.re.kr.

Notes

The authors declare no competing financial interest.

ACKNOWLEDGMENTS

This work was supported by the program funded by the Korea Institute of Science and Technology (KIST-2014-2E24662).

REFERENCES

(1) Wang, Q.; Luo, J.; Zhong, Z.; Borgna, A. CO_2 Capture by Solid Adsorbents and Their Applications: Current Status and New Trends. *Energy Environ. Sci.* **2011**, *4*, 42−55.

(2) Li, J. R.; Ma, Y.; McCarthy, M. C.; Sculley, J.; Yu, J.; Jeong, H. K.; Balbuena, P. B.; Zhou, H. C. Carbon Dioxide Capture-Related Gas Adsorption and Separation in Metal-Organic Frameworks. *Coord. Chem. Rev.* **2011**, *255*, 1791−1823.

(3) Alkhabbaz, M. A.; Khunsupat, R.; Jones, C. W. Guanidinylated Poly(allyamine) Supported on Mesoporous Silica for CO_2 Capture from Flue Gas. *Fuel* **2014**, *121*, 79−85.

(4) Yang, Z. Z.; He, L. N.; Gao, J.; Liu, A. H.; Yu, B. Carbon Dioxide Utilization with C-N Bond Formation: Carbon Dioxide Capture and Subsequent Conversion. *Energy Environ. Sci.* **2012**, *5*, 6602−6639.

(5) Choi, S.; Drese, J. H.; Jones, C. W. Adsorbent Materials for Carbon Dioxide Capture from Large Anthropogenic Point Sources. *ChemSusChem* **2009**, *2*, 796−854.

(6) Yue, M. B.; Chun, Y.; Cao, Y.; Dong, X.; Zhu, J. H. CO_2 Capture by As-Prepared SBA-15 with an Occluded Organic Template. *Adv. Funct. Mater.* **2006**, *16*, 1717−1722.

(7) Bhagiyalakshmi, M.; Yun, L. J.; Anuradha, R.; Jang, H. T. Utilization of Rice Husk Ash as Silica Source for the Synthesis of Mesoporous Silicas and Their Application to CO_2 Adsorption through TREN/TEPA Grafting. *J. Hazard. Mater.* **2010**, *175*, 928−938.

(8) Stuckert, N. R.; Yang, R. T. CO_2 Capture from the Atmosphere and Simultaneous Concentration Using Zeolites and Amine-Grafted SBA-15. *Environ. Sci. Technol.* **2011**, *45*, 10257−10264.

(9) Hicks, J. C.; Drese, J. H.; Fauth, D. J.; Gray, M. L.; Qi, G.; Jones, C. W. Designing Adsorbents for CO_2 Capture from Flue Gas-Hyperbranched Aminosilicas Capable of Capturing CO_2 Reversibly. *J. Am. Chem. Soc.* **2008**, *130*, 2902−2903.

(10) Sayari, A.; Belmabkhout, Y. Stabilization of Amine-Containing CO_2 Adsorbents: Dramatic Effect of Water Vapor. *J. Am. Chem. Soc.* **2010**, *132*, 6312−6314.

(11) Bhagiyalakshmi, M.; Yun, L. J.; Anuradha, R.; Jang, H. T. Synthesis of Chloropropylamine Grafted Mesoporous MCM-41, MCM-48 and SBA-15 from Rice Husk Ash: Their Application to CO_2 Chemisorption. *J. Porous Mater.* **2010**, *17*, 475−484.

(12) Amatani, T.; Nakanishi, K.; Hirao, K.; Kodaira, T. Monolithic Periodic Mesoporous Silica with Well-Defined Macropores. *Chem. Mater.* **2005**, *17*, 2114−2119.

(13) Kanamori, K.; Nakanishi, K. Controlled Pore Formation in Organotrialkoxysilane-Derived Hybrids: From Aerogels to Hierarchically Porous Monoliths. *Chem. Soc. Rev.* **2011**, *40*, 754−770.

(14) Hu, Y. S.; Adelhelm, P.; Smarsly, B. M.; Hore, S.; Antonietti, M.; Maier, J. Synthesis of Hierarchically Porous Carbon Monoliths with Highly Ordered Microstructure and Their Application in Rechargeable Lithium Batteries with High-Rate Capability. *Adv. Funct. Mater.* **2007**, *17*, 1873−1878.

(15) Nakanishi, K.; Kobayashi, Y.; Amatani, T.; Hirao, K.; Kodaira, T. Spontaneous Formation of Hierarchical Macro-Mesoporous Ethane-Silica Monolith. *Chem. Mater.* **2004**, *16*, 3652−3658.

(16) Brandhuber, D.; Peterlik, H.; Hüsing, N. Simultaneous Drying and Chemical Modification of Hierarchically Organized Silica Monolith with Organofunctional Silanes. *J. Mater. Chem.* **2005**, *15*, 3896−3902.

(17) Triantafillidis, C.; Elsaesser, M. S.; Hüsing, N. Chemical Phase Separation Strategies towards Silica Monoliths with Hierarchical Porosity. *Chem. Soc. Rev.* **2013**, *42*, 3833−3846.

(18) Nakanishi, K.; Tanaka, N. Sol-Gel with Phase Separation. Hierarchically Porous Materials Optimized for High-Performance Liquid Chromatography Separations. *Acc. Chem. Res.* **2007**, *40*, 863−873.

(19) Xue, C.; Wang, J.; Tu, B.; Zhao, D. Hierarchically Porous Silica with Ordered Mesostructure from Confinement Self-assembly in Skeleton Scaffolds. *Chem. Mater.* **2010**, *22*, 494−503.

(20) Xue, C.; Tu, B.; Zhao, D. Evaporation-Induced Coating and Self-Assembly of Ordered Mesoporous Carbon-Silica Composite Monoliths with Macroporous Architecture on Polyurethane Foams. *Adv. Funct. Mater.* **2008**, *18*, 3914−3921.

(21) Han, D.; Li, X.; Zhang, L.; Wang, Y.; Yan, Z.; Liu, S. Hierarchically Ordered Meso/Macroporous γ-Alumina for Enhanced Hydrodesulfurization Performance. *Microporous Mesoporous Mater.* **2012**, *158*, 1−6.

(22) Huang, Y.; Cai, H.; Feng, D.; Gu, D.; Deng, Y.; Tu, B.; Wang, H.; Webley, P. A.; Zhao, D. One-Step Hydrothermal Synthesis of Ordered Mesostructured Carbonaceous Monoliths with Hierarchical Porosities. *Chem. Commun.* **2008**, 2641−2643.

(23) Ek, S.; Iiskola, E. I.; Niinistö, L.; Vaittnen, J.; Pakkanen, T. T.; Keränen, J.; Auroux, A. Atomic Layer Deposition of a High-Density Aminopropylsiloxane Network on Silica through Sequential Reactions of γ-Aminopropyltrialkoxysilanes and Water. *Langmuir* **2003**, *19*, 10601−10609.

(24) Ko, Y. G.; Lee, H. J.; Oh, H. C.; Choi, U. S.; Amines, U. S. Immobilized Double-Walled Silica Nanotubes for CO_2 Capture. *J. Hazard. Mater.* **2013**, *250−251*, 53−60.

(25) Kristensen, E. M. E.; Nederberg, F.; Rensmo, H.; Bowden, T.; Hilborn, J.; Siegbahn, H. Photoelectron Spectroscopy Studies of the Functionalization of a Silicon Surface with a Phosphorylcholine-

Terminated Polymer Grafted onto (3-Aminopropyl)trimethoxysilane. *Langmuir* **2006**, *22*, 9651−9657.
(26) Acres, R. G.; Ellis, A. V.; Alvino, J.; Lenahan, C. E.; Khodakov, D. A.; Metha, G. F.; Andersson, G. G. Molecular Structure of 3-Aminopropyltriethoxysilane Layers Formed on Silanol-Terminated Silicon Surfaces. *J. Phys. Chem. C* **2012**, *116*, 6289−6297.
(27) Zhu, M.; Lerum, M. Z.; Chen, W. How to Prepare Reproducible, Homogeneous, and Hydrolytically Stable Aminosilane-Derived Layers on Silica. *Langmuir* **2012**, *28*, 416−423.
(28) Sing, K. S. W.; Everett, D. H.; Haul, R. A. W.; Moscou, L.; Pierotti, R. A.; Rouquérol, J.; Siemieniewska, T. Reporting Physisorption Data for Gas/Solid Systems with Special Reference to the Determination of Surface Area and Porosity. *Pure Appl. Chem.* **1985**, *57*, 603−619.
(29) Zhao, D.; Feng, J.; Huo, Q.; Melosh, N.; Fredrickson, G. H.; Chmelka, B. F.; Stucky, G. D. Triblock Copolymer Syntheses of Mesoporous Silica with Periodic 50 to 300 Angstrom Pores. *Science* **1998**, *279*, 548−552.
(30) Yokoi, T.; Yoshitake, H.; Tatsumi, T. Synthesis of Amino-Functionalized MCM-41 via Direct Co-Condensation and Post-Synthesis Grafting Methods Using Mono-, Di- and Tri-Amino-Organoalkoxysilanes. *J. Mater. Chem.* **2004**, *14*, 951−957.
(31) Heydari-Gorji, A.; Belmabkhout, Y.; Sayari, A. Polyethyleneimine-Impregnated Mesoporous Silica: Effect of Amine Loading and Surface Alkyl Chains on CO_2 Adsorption. *Langmuir* **2011**, *27*, 12411−12416.
(32) Ko, Y. G.; Shin, S. S.; Choi, U. S. Primary, Secondary, and Tertiary Amines for CO_2 Capture: Designing for Mesoporous CO_2 Adsorbents. *J. Colloid Interface Sci.* **2011**, *361*, 594−602.
(33) Caplow, M. Kinetics of Carbamate Formation and Breakdown. *J. Am. Chem. Soc.* **1968**, *90*, 6795−6803.
(34) Hiyoshi, N.; Yogo, K.; Yashima, T. Adsorption Characteristics of Carbon Dioxide on Organically Functionalized SBA-15. *Microporous Mesoporous Mater.* **2005**, *84*, 357−365.
(35) Knöfel, C.; Martin, C.; Hornebecq, V.; Liewllyn, P. L. Study of Carbon Dioxide Adsorption on Mesoporous Aminopropylsilane-Functionalized Silica and Titania Combining Microcalorimetry and in Situ Infrared Spectroscopy. *J. Phys. Chem. C* **2009**, *113*, 21726−21734.
(36) Bacsik, Z.; Ahlsten, N.; Ziadi, A.; Zhao, G.; Garcia-Bennett, A. E.; Martín-Matute, B.; Hedin, N. Mechanisms ad Kinetics for Sorption of CO_2 on Bicontinuous Mesoporous Silica Modified with *n*-Propylamine. *Langmuir* **2011**, *27*, 11118−11128.
(37) Danon, A.; Stair, P. C.; Weitz, E. FTIR Study of CO_2 Adsorption on Amine-Grafted SBA-15: Elucidation of Adsorbed Species. *J. Phys. Chem. C* **2011**, *115*, 11540−11549.
(38) Zheng, F.; Tran, D. N.; Busche, B. J.; Fryxell, G. E.; Addleman, R. S.; Zemanian, T. S.; Aardahl, C. L. Ethylenediamine-Modified SBA-15 as Regenerable CO_2 Sorbent. *Ind. Eng. Chem. Res.* **2005**, *44*, 3099−3105.
(39) Goeppert, A.; Czaun, M.; May, R. B.; Prakash, G. K. S.; Olah, G. A.; Narayanan, S. R. Carbon Dioxide Capture from the Air Using a Polyamine Based Regenerable Solid Adsorbent. *J. Am. Chem. Soc.* **2011**, *133*, 20164−20167.
(40) Ma, X.; Wang, X.; Song, C. Molecular Basket" Sorbents for Separation of CO_2 and H_2S from Various Gas Streams. *J. Am. Chem. Soc.* **2009**, *131*, 5777−5783.
(41) Ojuva, A.; Akhtar, F.; Tomsia, A. P.; Bergström, L. Laminated Adsorbents with Very Rapid CO_2 Uptake by Freeze-Casting of Zeolites. *ACS Appl. Mater. Interfaces* **2013**, *5*, 2669−2676.
(42) Chen, C.; Yang, S.-T.; Ahn, W.-S.; Ryoo, R. Amine-Impregnated Silica Monolith with a Hierarchical Pore Structure: Enhancement of CO_2 Capture Capacity. *Chem. Commun.* **2009**, 3627−3629.
(43) Yu, J.; Su, Y.; Cheng, B. Template-Free Fabrication and Enhancement Photocatalytic Activity of Hierarchical Macro-/Mesoporous Titania. *Adv. Funct. Mater.* **2007**, *17*, 1984−1990.
(44) Smått, J.-H.; Schunk, S.; Lindén, M. Versatile Double-Templating Synthesis Route to Silica Monoliths Exhibiting a Multimodal Hierarchical Porosity. *Chem. Mater.* **2003**, *15*, 2354−2361.
(45) Hasan, F. A.; Xiao, P.; Singh, R. K.; Webley, P. A. Zeolite Monoliths with Hierarchical Designed Pore Network Structure: Synthesis and Performance. *Chem. Eng. J.* **2013**, *223*, 48−58.